JOC The Journal of Organic Chemistry

Article

pubs.acs.org/joc

Synthesis and Characterization of PEGylated Trityl Radicals: Effect of PEGylation on Physicochemical Properties

Wenbo Liu,[†] Jiangping Nie,[†] Xiaoli Tan,[†] Huiqiang Liu,[†] Nannan Yu,[†] Guifang Han,[†] Yutian Zhu,[#] Frederick A. Villamena,[§] Yuguang Song,[†] Jay L. Zweier,*[,‡] and Yangping Liu*[,†,‡]

[†]Tianjin Key Laboratory on Technologies Enabling Development of Clinical Therapeutics and Diagnostics, School of Pharmacy, Tianjin Medical University, Tianjin 300070, P. R. China

[‡]Center for Biomedical EPR Spectroscopy and Imaging, The Davis Heart and Lung Research Institute, the Division of Cardiovascular Medicine, Department of Internal Medicine, The Ohio State University, Columbus, Ohio 43210, United States

[#]State Key Laboratory of Polymer Physics and Chemistry, Changchun Institute of Applied Chemistry, Chinese Academy of Sciences, Changchun 130022, P. R. China

[§]Department of Biological Chemistry and Pharmacology, College of Medicine, The Ohio State University, Columbus, Ohio 43210, United States

Supporting Information

ABSTRACT: Tetrathiatriarylmethyl (TAM, trityl) radicals have attracted considerable attention as spin probes for biological electron paramagnetic resonance (EPR) spectroscopy and imaging owing to their sharp EPR singlet signals and high biostability. However, their *in vivo* applications were limited by the short blood circulation lifetimes and strong binding with albumins. Our previous results showed that PEGylation is a feasible method to overcome the issues facing *in vivo* applications of TAM radicals. In the present study, we synthesized a series of new PEGylated TAM radicals (TTP1, TPP2, TNP1, TNP2, d-TNP1, and d-TNP3) containing various lengths and numbers of mPEG chains. Our results found that the pattern of PEGylation exerts an important effect on physicochemical properties of the resulting TAM radicals. Dendritic PEGylated TAM radicals, TNP1 and TNP2, have higher water solubility and lower susceptibility for self-aggregation than their linear analogues TPP1 and TPP2. Furthermore, dendritic PEGylated TAM radicals exhibit extremely high stability toward various biological oxidoreductants as well as in rat whole blood, liver homogenate, and following *in vivo* intravenous administration in mice. Importantly, the deuterated derivatives, especially d-TNP3, exhibit excellent properties including the sharp and O_2-sensitive EPR singlet signal, good biocompatibility, and prolonged kinetics with half-life time of ≥10 h in mice. These PEGylated TAM radicals should be suitable for a wide range of applications in *in vivo* EPR spectroscopy and imaging.

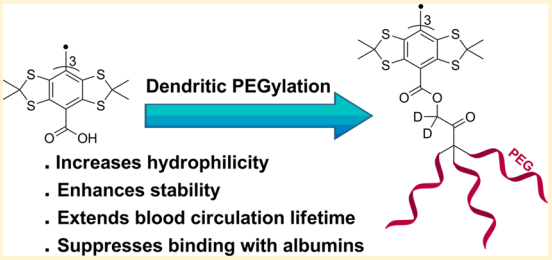

1. INTRODUCTION

Stable organic radicals are of prime interest owing to their diverse applications in the fields of chemistry, material, and biomedical sciences. Triphenylmethyl radical is the first organic free radical which was synthesized by Gomberg in 1900.[1] However, its use, especially in biomedical applications, was limited due to low stability and/or low water-solubility. To address these issues, tetrathiatriarylmethyl (TAM, trityl) radicals which belong to a family of fully substituted triphenylmethyl radicals were developed.[2,3] Full substitution of each phenyl ring in TAM radicals by alkylthio and carboxylate groups not only eliminates hyperfine splittings from protons but also increases their stability and water solubility, thus expanding their applications in biological magnetic resonance spectroscopy. The most well-studied members of TAM radicals are CT-03 and its more hydrophilic analogue OX063, both of which contain three carboxyl groups in their molecular structures (Chart 1).

Besides high stability and water solubility, TAM radicals also have long relaxation times (>10 μs at 25 °C under anaerobic conditions) and narrow electron paramagnetic resonance (EPR) singlet signals which provide high sensitivity and resolution for EPR imaging. Owing to these unique properties, these radicals have been widely utilized in continuous-wave and pulsed EPR spectroscopy and imaging[4,5] as well as magnetic resonance imaging and other related fields.[6−10] The great demand for TAM radicals has stimulated numerous efforts toward optimization of synthetic strategies, thus resulting in the practical and large-scale synthesis of CT-03.[11,12] The novel synthetic method based on nucleophilic quenching of the TAM cation was also reported for the challenging asymmetric TAM radicals.[13,14] Fluorinated TAMs with a high affinity to fluorous media were developed in order to evaluate tumor oxygenation

Received: October 26, 2016
Published: December 22, 2016

DOI: 10.1021/acs.joc.6b02590
J. Org. Chem. 2017, 82, 588−596

Chart 1. Molecular Structures of TAM Radicals

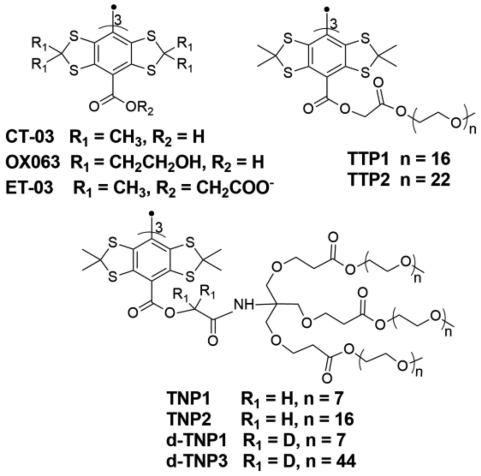

using biocompatible perfluorocarbon emulsions.[15,16] Furthermore, peptide-conjugated[17,18] and esterified TAM radicals[19,20] have enabled intracellular targeting. On the other hand, TAM radicals have been structurally modified to expand their applications for measurement of physiological parameters such as superoxide anion radical ($O_2^{\bullet-}$),[21] pH,[22−24] thiol levels[25] as well as total redox status.[26] Most recently, these radicals and their derivatives also have shown great promise as spin labels for distance measurements in proteins and nucleic acids by pulsed EPR spectroscopy at physiological temperature[27,28] and as efficient polarizing agents of high-field dynamic nuclear polarization.[29]

Despite the fact that TAM radicals have excellent properties allowing for their wide applications in various fields of research, short blood circulation lifetime and strong binding with albumins still limit their *in vivo* applications.[6,30] Potential toxicity of CT-03 resulting from relatively high hydrophobicity and strong binding with proteins is another limitation for its biological applications.[4,31] Thus, OX063, the hydrophilic analogue of CT-03, is commonly used in the magnetic resonance-related field.[7] However, the synthesis of OX063 with high yield is still a challenge and this synthesis has only been reported in the patent literature until now.[32−34] In addition OX063 has a very short *in vivo* half-life with rapid renal clearance from the body.[35] Comparatively, the synthesis of CT-03 is easier and its large-scale synthesis has been achieved as reported previously.[3,11]

In order to overcome the drawbacks of CT-03, much effort has been made to encapsulate it into oily core nanocapsules[36] or Pluronic F-127 hydrogel.[37] The resulting nanoformulations of TAM radicals exhibited improved biocompatibility and high stability with long *in vivo* half-life times, thus showing great potential for *in vivo* utilization in EPR spectroscopy and imaging. In the meantime, we have been searching for new covalent derivatization strategies in the past years to overcome the disadvantages of CT-03 without compromising its excellent EPR properties. As such, we reported the synthesis of a dendritic esterified form of CT-03 which was able to be further conjugated with methoxypolyethylene glycol (mPEG) chains at the terminal carboxylic groups.[30] The resulting PEGylated TAM radical exhibits negligible albumin binding, high oxygen (O_2) sensitivity, and potentially long blood circulation time.[30] PEGylation has been an effective strategy to promote targeting delivery of biologically active small molecules and proteins and enhance their biocompatibility and stability.[38−41] Similar results have also been reported for PEGylated organic radical contrast agents that have long *in vivo* half-life and good biocompatibility, thus showing great potentials for magnetic resonance imaging.[42,43] However, it is not clear how the length and number of mPEG chains affect the physicochemical properties of CT-03 derivatives. Moreover, it was challenging to achieve full PEGylation of nine carboxylic groups in the dendritic TAM radical using the previous synthetic approach. Therefore, in the present study, we utilized a completely convergent method to synthesize PEGylated CT-03 derivatives TTP1, TTP2, TNP1, and TNP2 (Chart 1), which contain different mPEG chain lengths (MW 350−2000) and numbers (3/9 chains). This new

Scheme 1. Synthesis of PEGylated Monomers

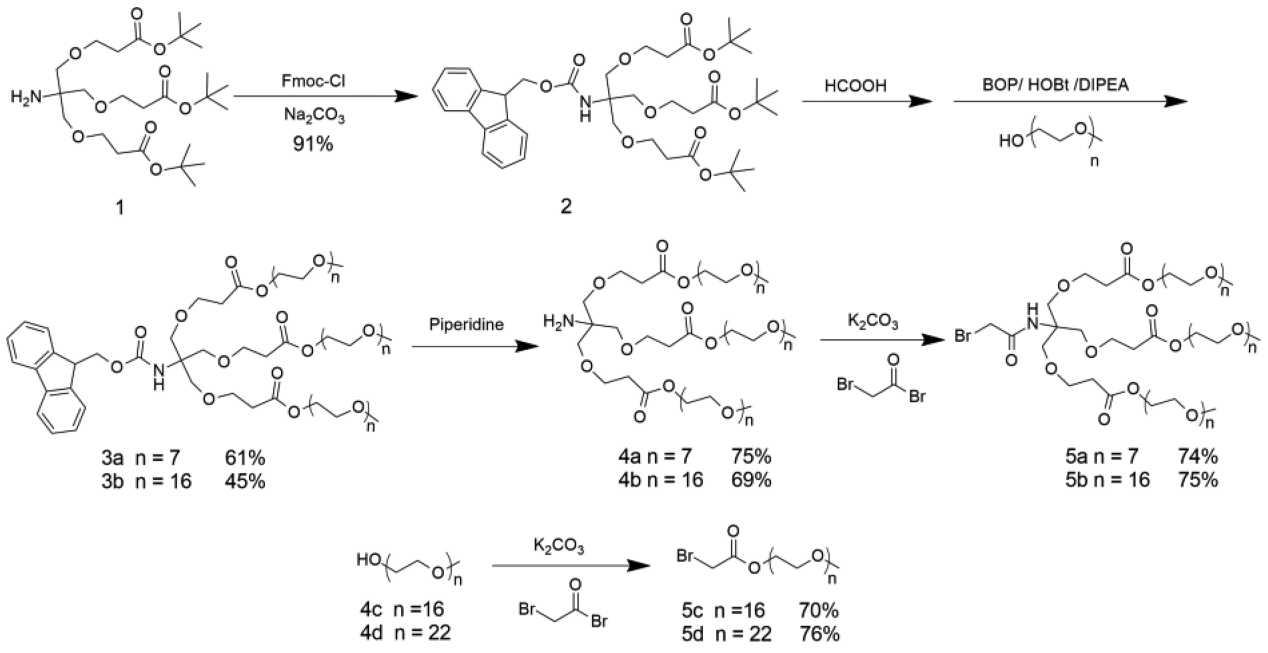

DOI: 10.1021/acs.joc.6b02590
J. Org. Chem. 2017, 82, 588−596

Scheme 2. Synthesis of PEGylated TAM Radicals

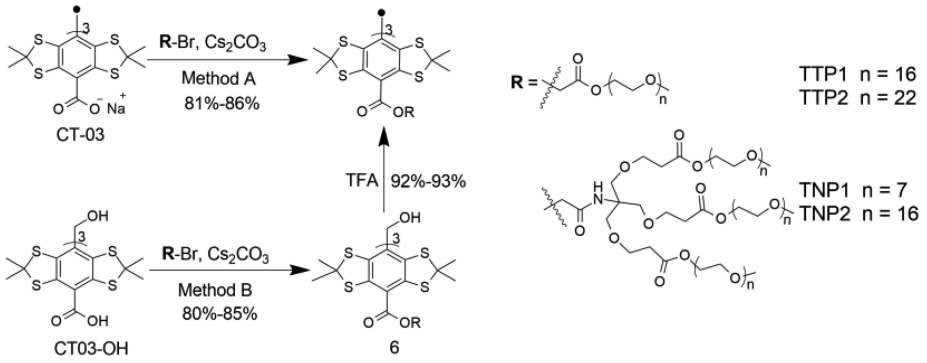

convergent method allows for full PEGylation of all of carboxylic acids. The resulting PEGylated TAM radicals were characterized by UV−vis, ^{1}H NMR, matrix-assisted laser desorption ionization-time-of-flight (MALDI-TOF), and EPR. The self-aggregation concentration, hydrophobicity, O_2 sensitivity, and binding with bovine serum albumin of these radicals were compared for these new radicals. Their stability toward various oxidoreductants as well as in rat liver homogenate and whole blood were also studied. In addition, the deuterated derivatives d-TNP1 and d-TNP3 were also synthesized, and the *in vivo* biocompatibility and kinetics of d-TNP3 were evaluated in mice.

2. RESULTS AND DISCUSSION

2.1. Synthesis. *2.1.1. Synthesis of PEGylated Monomers.* The PEGylated monomers **4a** and **4b** were synthesized through a three-step procedure shown in Scheme 1. The Fmoc-protected dendron **2** was obtained by reaction of the trifurcated Newkome-type compound **1** with Fmoc-Cl in the presence of Na_2CO_3 as reported previously.[44] After deprotection by formic acid, the dendron **2** was then coupled with methoxypolyethylene glycols (mPEGs) 350 and 750 (average molecular weight) to result in the dendrons **3a** and **3b**, respectively. Finally, the PEGylated monomers **5a** and **5b** were obtained by deprotection with piperidine, followed by reaction with bromoacetyl bromide in the presence of K_2CO_3. On the other hand, the monomers **5c** and **5d** were easily obtained by direct conjugation of mPEG 350 and 750 with bromoacetyl bromide in the presence of K_2CO_3.

2.1.2. Synthesis of PEGylated TAM Radicals. The PEGylated TAM radicals were obtained using two different methods (Scheme 2). In method A, CT-03 reacted with excess of the PEGylated monomers **5a−5d** to afford the PEGylated TAM radicals TNP1, TNP2, TTP1, and TTP2. In method B, the nonradical precursor of CT-03 (CT03-OH)[45] reacted with excess of the PEGylated monomers **5a−5d** to yield compound **6**, which was further transformed into the corresponding PEGylated TAM radicals upon treatment by TFA.[46]

Comparison of these two synthetic methods shows that the method A is much more facile with higher yields (81−86%) due to one less step than the method B (74−78%). However, since the paramagnetism of TAM radicals can significantly broaden NMR signals of protons close to the radical center, PEGylated TAM radicals can be not completely characterized by NMR. Therefore, the corresponding nonradical analogues **6** are very useful to provide the structural information on PEGylated TAM radicals.

2.2. ^{1}H NMR Studies. ^{1}H NMR spectra of TNP1 and its nonradical form TNP1-OH were recorded in both $CDCl_3$ and D_2O at room temperature (Figure 1 and the Supporting Information for the complete spectra). As shown in Figure 1A, the spectrum of TNP1-OH in $CDCl_3$ shows three proton resonances between 1.69 and 1.87 ppm with an integration peak intensities ratio of 1:1:2. These upfield peaks can be assigned to four methyl groups on six five-membered side rings which exhibit four separate and equal-intensity peaks for other TAM derivatives.[45] One less peak at the region of 1.69−1.87 ppm was observed for TNP1-OH which was most likely due to linkage of the large PEGylated dendrons that results in slow rotational motions. Similar results were also observed when ^{1}H NMR spectrum of a non-PEGylated analogue of TNP1-OH was recorded in viscous d6-DMSO instead of in $CDCl_3$. On the other hand, the signals (3.63−3.73 ppm) due to protons in the mPEG group (CH_2CH_2O) can be utilized to estimate the length of the mPEG chain. It was determined that there were approximately 7 repeating units of CH_2CH_2O in each mPEG chain and the estimated molecular weight (~340 Da) of the mPEG chain is consistent with its average value (350 Da).

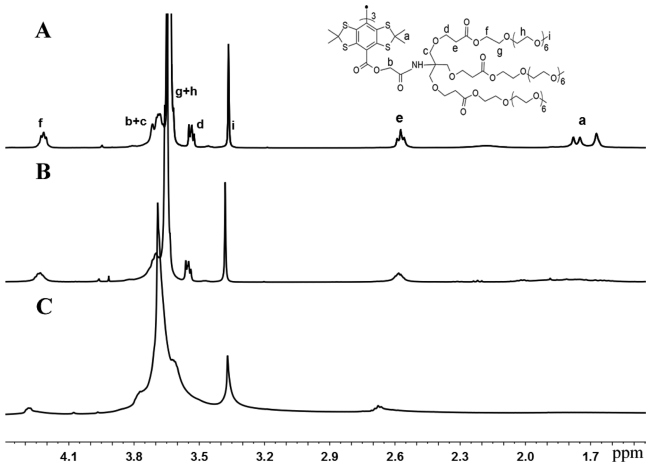

Figure 1. ^{1}H NMR spectra of (A) TNP1-OH in $CDCl_3$, (B) TNP1 in $CDCl_3$, and (C) TNP1 in D_2O.

Since the paramagnetic nature of TAM radicals can broaden NMR signals in close proximity to the central spin, comparison of ^{1}H NMR spectra of TNP1 and TNP1-OH can provide valuable information about their conformations in solution. As shown in Figure 1B, the peaks (H_a) at the region of 1.69−1.87 ppm in ^{1}H NMR spectrum of TNP1 in $CDCl_3$ almost completely vanished due to the strong broadening induced by

DOI: 10.1021/acs.joc.6b02590
J. Org. Chem. 2017, 82, 588−596

the central spin. Moreover, the signals at 2.65 (H_e) and 4.25 (H_f) ppm were moderately broadened such that these triplets were unresolved possibly due to the spatial proximity to the TAM core induced by back folding of the corresponding ester part. Similar line broadening was also observed for partial protons (3.63−3.73 ppm) on ethylene glycol repeat units. Interestingly, multiplet signal from H_d at 3.55 ppm was still well resolved without significant broadening although the H_d protons are in closer proximity to the central spin than both H_e and H_f protons, further confirming that the part containing H_e and H_f protons was backward folded to the central spin. As expected, the terminal methyl groups of mPEG chain in the ^{1}H NMR spectrum of TNP1 have as sharp a singlet signal as that in TNP1-OH due to their spatially distant separation from the central TAM core. On the basis of the above observations, it can be visualized that dendritic mPEG chains in TNP1 are partially back-folded to the TAM core in $CDCl_3$ and provide protection to the latter.

In order to reveal if there is similar dendritic encapsulation in TNP1 in aqueous solution, its ^{1}H NMR spectrum was also recorded in D_2O and compared with that in $CDCl_3$. As shown in Figure 1C, all of the NMR signals in D_2O were much broadened relative to the corresponding signals in $CDCl_3$, most likely due to self-aggregation of TNP1 at high concentration (~2.38 mM) in D_2O (see below). However, careful examination revealed that the signals of H_e and H_f become much broader in D_2O than those in $CDCl_3$, possibly because H_e and H_f were closer to the paramagnetic TAM core in D_2O than in $CDCl_3$. In addition, in contrast to the spectrum in $CDCl_3$, the signal of the protons H_d in D_2O was very broad and completely buried into the signals of mPEG units or into the baseline. Therefore, the protons H_d, H_e and H_f are much closer to the TAM core in D_2O than in $CDCl_3$, indicative of a stronger protection to the TAM core provided by the dendritic PEGylation in D_2O. The strong protection is also further verified by their high stability toward various reactive species (see below).

2.3. UV−vis Spectroscopic Studies. *2.3.1. UV−vis Absorption.* Data on UV−vis absorption are shown in Table 1. In phosphate buffer (PB), the non-PEGylated TAM radical

Table 1. UV−vis Absorption and Octanol-Water Partition Coefficients (logP) of TAM Radicals in Phosphate Buffer (PB, 20 mM, pH 7.4) and DMSO/PB (v/v = 1:1)

radical	solvent	λ_{max}/nm (ε/mM^{-1} cm^{-1})[b]	logP[c]
ET-03	PB[a]	400 (14.4), 484 (15.3), 662	−0.11 ± 0.03
TNP1	PB[a]	418 (21.6), 496 (20.1), 692	−1.27 ± 0.02
	DMSO-PB[d]	418 (25.6), 496 (24.3), 692	
TNP2	PB[a]	418 (20.4), 496 (19.4), 692	−1.49 ± 0.02
	DMSO-PB[d]	418 (25.5), 496 (24.7), 692	
TTP1	DMSO-PB[d]	418 (25.2), 496 (24.2), 692	−0.19 ± 0.01
TTP2	DMSO-PB[d]	418 (25.7), 496 (24.6), 692	−1.34 ± 0.04

[a]Phosphate buffer. [b]ε, molar extinction coefficient (see more details in Figure S5). [c]Octanol−water partition coefficient (see more details in Table S4). [d]DMSO/PB (v/v = 1:1).

ET-03 (Chart 1) displayed two intense and characteristic UV−vis absorption bands around 400 and 484 nm and a broad and weak band around 662 nm due to the n → π^* transition. These absorption bands were blue-shifted relative to the previously reported esterified TAM radicals (408, 491, and 682 nm) possibly because of the stronger inductive effect from the ester groups in ET-03.[47] The dendritic PEGylated TAM radicals TNP1 and TNP2 exhibited almost identical UV−vis spectra (Figure S5) with λ_{max} values at ~418, 496, and 692 nm in PB which were red-shifted as compared to the corresponding peaks in ET-03 and other esterified TAM radicals.[47] Addition of DMSO (50%) into the solutions of TNP1 and TNP2 did not induce red-shift in their maximal UV−vis absorptions (Table 1) but increased their molar extinction coefficients (ε) from ~20 to 25 mM^{-1} cm^{-1} at both 400 and 496 nm. In order to prevent potential self-aggregation (see section 2.3.2 Self-Aggregation Behavior below), UV−vis spectra of linear PEGylated TAM radicals TTP1 and TTP2 were only recorded in DMSO/PB (v/v = 1:1). Both of them exhibited very similar ε and λ_{max} values with TNP1 and TNP2 in DMSO/PB, indicating that the number and length of PEG chains have no significant effect on the UV−vis spectra of PEGylated TAM radicals.

2.3.2. Octanol−Water Partition Coefficient (logP). Knowledge about hydrophilicity/hydrophobicity of TAM radicals is helpful to predict their potential for *in vivo* application. As shown in Table 1, although ET-03 contains three charged carboxylate groups in its molecule, it still exhibits moderate distribution in the octanol layer with a logP value of −0.11. Dendritic PEGylations significantly increase the hydrophilicity of TNP1 (logP = −1.27) and TNP2 (logP = −1.49). TTP2 with relatively longer and linear mPEG chains (MW = 1000) has significantly higher hydrophilicity (logP = −1.34) than TTP1 with shorter and linear mPEG chains (MW = 750, logP = −0.19). Therefore, increasing the mPEG length and number can effectively improve the hydrophilicity of PEGylated TAM radicals.

2.4. EPR Studies. *2.4.1. Hyperfine Splitting Constants.* Under anaerobic conditions, ET-03 exhibits an ambiguous EPR multiplet signal (Figure 2) due to interaction of the unpaired

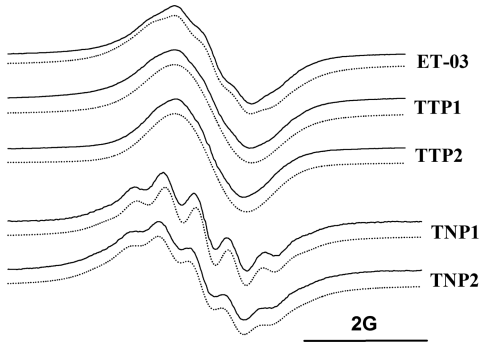

Figure 2. Experimental (solid line) and simulated (dotted line) EPR spectra of ET-03 (100 μM), TNP1 (100 μM), and TNP2 (100 μM) in phosphate buffer (PB, 20 mM, pH 7.4), TTP1 (100 μM), and TTP2 (100 μM) in DMSO/PB (v/v = 1:1) under anaerobic conditions. EPR instrument settings were as follows: modulation frequency, 30 kHz; microwave frequency, 9.87 GHz; microwave power, 0.1 mW; modulation amplitude, 0.02 G.

electron with six protons of three ester groups through extensive π conjugation and hyperconjugation along the central carbon, aryl groups, and ester groups. Slightly different hyperfine splitting constants (α_H) of 65 and 70 mG (Table 2) for the two protons from each methylene group of ET-03 were observed which could originate from the hindered rotation of the para substitutents and the intrinsic chirality of the TAM core as described previously.[48] The measured α_H values for ET-03 were very similar to the previously reported

DOI: 10.1021/acs.joc.6b02590
J. Org. Chem. 2017, 82, 588−596

Table 2. EPR Properties of TAM Radicals in Phosphate Buffer (20 mM, pH 7.4) under Anaerobic and Aerobic Conditions

		ΔB_{pp}/mG[b]			line width/mG[d]			
radical	α_H/mG (n[a])	An[c]	air	ratio[b]	An[c]	air	ratio[d]	SAC/μM[e]
ET-03	65 (3), 70 (3)	211	321	1.52	90	130	1.44	500
TTP1	70(3), 75 (3)	219	305	1.39	90	120	1.33	10
TTP2	70 (3), 75 (3)	217	304	1.40	92	120	1.30	11
TNP1	85 (3), 87 (3)	254	351	1.38	90	110	1.22	250
TNP2	85(3), 87 (3)	259	352	1.35	95	120	1.26	230
d-TNP1		120	226	1.88				ND[f]
d-TNP3		130	230	1.77				ND[f]

[a]The number of equivalent H nuclei. [b]The ratio of peak-to-peak line widths (ΔB_{pp}) under aerobic and anaerobic conditions. [c]Anaerobic. [d]The ratio of intrinsic line widths under aerobic and anaerobic conditions. [e]SAC, self-aggregation concentration. [f]ND, not determined. The standard derivations of α_H, ΔB_{pp}, and line width are <5 mG.

value (70 mG).[46] Direct esterification of ET-03 with the linear mPEG chains enhances the interaction of the unpaired electron with the six protons as evidenced by the slightly higher α_H values (70 and 75 mG) for TTP1 and TTP2. Both TTP1 and TTP2 have completely unresolved multiplet signals due to the relatively small α_H values but large line widths (~90 mG). Conversely, EPR spectra of TNP1 and TNP2 consist of explicit multiplets with α_H values of 85 and 87 mG and line widths of ~90 mG.

2.4.2. Self-Aggregation Behavior. Since the line broadening induced by intermolecular spin−spin interaction may interfere with the O_2-induced broadening and thus could complicate the interpretation of results obtained from application of TAM radicals for measurement of O_2, we investigated the effect of concentration of PEGylated TAM radicals on their EPR signals. As expected, the signal intensity of TAM radicals increases linearly with concentrations. However, this relationship deviates from the linearity above the self-aggregation concentrations (SACs), because the intermolecular spin−spin interaction induced by the self-aggregation broadens the signals and thus decreases their signal intensity (Figure S8). As shown in Table 2, among the five TAM radicals studied, ET-03 has the highest SAC value (500 μM) possibly because the intermolecular static repulsion from the charged carboxylate groups effectively prevents their self-aggregation. The conjugation of linear mPEG chains to TAM radicals through the ester linkage leads to a rapid reduction of their SACs (10 μM for TPP1 and 11 μM for TTP2). However, dendritic PEGylation is very beneficial to prevent the self-aggregation of TAM radicals based on the following facts: (1) SACs of both TNP1 (250 μM) and TNP2 (225 μM) are much higher than those of TTP1 (10 μM) and TTP2 (11 μM); (2) TNP1 and TTP2 with the similar accumulative mPEG chain lengths (3 × 3 × 350 = 3150 Da for TNP1 and 3 × 1000 = 3000 Da for TTP2) have entirely different SACs with much higher value for the former (Table 2). Similar results were also observed in a previous study where dendritic encapsulation has been shown to prevent self-aggregation of dye molecules.[49] The almost identical SAC values for TPP1 vs TTP2 or TNP1 vs TNP2 (Table 2) indicate that the mPEG chain number instead of their length plays a significant role on the self-aggregation behavior of PEGylated TAM radicals.

2.4.3. Sensitivity of EPR Line Width to O_2. To evaluate the O_2 sensitivity of PEGylated TAM radicals, their EPR spectra were recorded under both anaerobic (Figure 2) and aerobic conditions (Figure S7), and their intrinsic EPR line widths of multiplets and peak-to-peak line widths (ΔB_{pp}) were obtained. The ratio of the two different kinds of line widths under two different conditions was used as an indicator for O_2 sensitivity of TAM radicals. As shown in Table 2, all PEGylated TAM radicals possess similar O_2 sensitivities with a ~1.3-fold increase in their intrinsic line widths from anaerobic to aerobic conditions. Similar results were also found for the ratios of ΔB_{pp} under different conditions, which are in the range of 1.35 to 1.40 and slightly higher than the ratios of the intrinsic line widths. The fact that ET-03 has the relatively higher ratio of ΔB_{pp} (1.52) than both linear and dendritic PEGylated TAM radicals is due to the presence of higher α_H values (~85 mG) for PEGylated TAM radicals than ET-03 (~55 mG), which results in attenuation of O_2 sensitivity.[30] As such, deuteration of the protons in the ester linker can sharpen EPR lines of TAM radicals and thus enhance their O_2 sensitivity.[30] Therefore, a deuterated analogue of TNP1, d-TNP1, was synthesized using the same synthetic procedure for TNP1 (Scheme 2) with the deuterated dendron of **4a** (Scheme 1). As expected, the deuteration greatly narrowed down the EPR signal of d-TNP1 (Figure S9) with a ΔB_{pp} value of 120 mG as compared to 254 mG for TNP-1 under anaerobic conditions. Accordingly, the ratio of ΔB_{pp} values (i.e., O_2 sensitivity) for d-TNP1 under aerobic and anaerobic conditions was significantly increased with a value of 1.88. Likewise, the other deuterated derivative d-TNP3 has similar O_2 sensitivity with d-TNP1 with the ΔB_{pp} ratio of 1.77 (Figure S10).

2.5. Stability in Rat Liver Homogenate and Blood. The stability of PEGylated TAM radicals toward various biological oxidoreductants was initially investigated. As shown in Table S2, all PEGylated TAM radicals show high stability toward these reactive species, especially for oxidants. For example, while the paramagnetism of CT-03 was quenched to different degrees by hydroxyl, peroxyl, and superoxide radicals, PEGylated TAM radicals have only less than 5% signal attenuation after 30 min incubation with these oxidants (Table S3). PEGylated encapsulation, especially with dendritic features, therefore provides marked protection to the TAM radicals, consistent with previous results from other dendritic TAM radicals.[30]

Previous studies showed that TAM radicals such as CT-03 can be rapidly metabolized in rat liver.[47,50] To test the metabolic stability of newly synthesized TAM radicals, CT-03, ET-03 (Chart 1), or d-TNP1 were incubated with fresh rat liver homogenate and the percentage of their EPR signal double-integration intensities remaining after 6 h of incubation in rat liver homogenate were compared. As shown in Figure 3, metabolism of CT-03 and ET-03 in rat liver homogenate was measured with 85% and 87%, respectively, of the signal intensities remaining after the incubation for 6 h. Conversely,

DOI: 10.1021/acs.joc.6b02590
J. Org. Chem. 2017, 82, 588−596

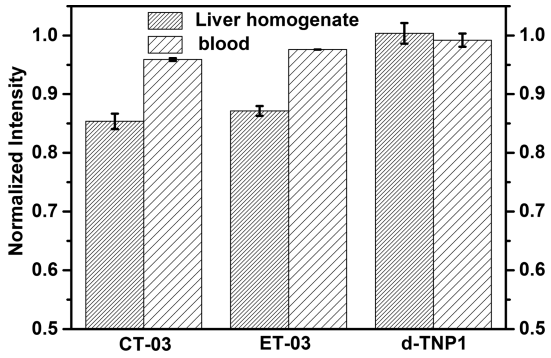

Figure 3. Stability of PEGylated TAM radical in rat liver homogenate and blood as a fraction of CT-03, ET-03, and d-TNP1 remaining after incubation for 6 h. The percentage was obtained by comparing the double integral of the EPR signal in each system with that of each radical (20 μM). Each experiment was carried out at least three times. See details in the Experimental Section.

the double-integration signal intensity of d-TNP1 remained almost unchanged during this period. Meanwhile, the EPR signal of d-TNP1 in rat liver homogenate became slightly sharper than that in phosphate buffer due to the O_2 consumption by active mitochondria in the homogenate as well as slow diffusion of air into the EPR capillary (Figure S11). These data showed that d-TNP1 has much higher resistance to liver metabolism than CT-03 and ET-03.[30]

To further explore *in vivo* application potential of dendritic PEGylated TAM radicals, the stability of d-TNP1 in whole blood from rat was also investigated. As shown in Figure 3, d-TNP1 showed high stability with less than 1% signal attenuation after 6 h incubation in the blood. Slightly lower stabilities were observed for CT-03 and ET-03. Importantly, the EPR signal of d-TNP1 did not show any significant change in the blood (Figure S12), whereas EPR signals of both CT-03 and ET-03 in the blood were severely broadened with less than 30% of signal intensities than those in phosphate buffer, most likely due to strong binding with plasma proteins.[31] To further confirm this assumption, the binding of those PEGylated TAM radicals with BSA was investigated. As expected, TNP1, TNP2, TTP1, and TTP2 did not bind to BSA (0–500 μM, Figure S13). Taken together, the dendritic PEGylation improves the biostability of TAM radicals in rat blood and enhances their *in vivo* application potential as EPR oximetric probes.

2.6. Evaluation of *in Vivo* Biocompatibility and Kinetics of d-TNP3. In order to test the biocompatibility and *in vivo* kinetics of PEGylated TAM radicals, d-TNP3 with long PEG chains (2 000 MW) was chosen for further study in mice. We performed measurements with intravenous administration and simultaneous L-band *in vivo* EPR measurements of the signal in the upper leg of mice. EPR measurements showed that fast uptake occurred in the leg reaching close to maximum within 2 min after the end of the infusion followed by a gradual further increase and then slow decay (Figure 4). Prolonged retention of the probe was achieved with stable EPR signal with less than 10% decay over 2 h, and the half-life of the observed signal was estimated to be ≥10 h. On the basis of the O_2-dependent line width broadening measured, the $[O_2]$ was measured as 65 μM, equivalent to a partial pressure of 43 Torr, in the upper leg muscles and this value remained stable for the period of measurement. Thus, compared to the original TAM probes, CT-03 or OX063,[7] d-TNP3 has greatly prolonged kinetics with good biocompatibility. In 4 mice studied, similar

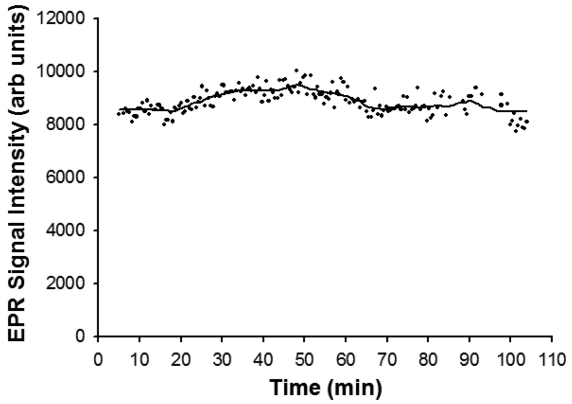

Figure 4. Time course of EPR signal intensity of d-TNP3 in the *in vivo* mouse. L-band EPR measurements were performed in the right upper leg of the mouse with surface coil resonator in mice infused with ~0.2 mmol/kg of d-TNP3 by intravenous infusion. The EPR signal was stable with little change over 2 h. There was no acute toxicity and the mice survived the infusion and measurements.

results were obtained with no acute adverse effects or toxicity noted. The mice survived for 3 days post probe infusion without problem and then were sacrificed with no abnormalities seen on gross pathology examination of the major organs.

3. CONCLUSIONS

We have developed a new class of PEGylated TAM radicals (TTP1, TTP2, TNP1, TNP2, d-TNP1, and d-TNP3) containing various lengths and numbers of mPEG chains. The number of mPEG chains but not their length has an important influence on the physicochemical properties of PEGylated TAM radicals. TNP1 and TNP2 with dendritic PEGylation exhibit better water solubility, less susceptible self-aggregation, higher stability in various systems than TTP1 and TTP2 with linear PEGylation while both types of PEGylated TAM radicals share similar and negligible BSA binding properties. The deuterated derivatives d-TNP1 and d-TNP3 have sharp and O_2-sensitive EPR singlet signals. Importantly, d-TNP3 exhibits excellent *in vivo* properties in mice including fast uptake, good biocompatibility, and prolonged kinetics with half-life time of ≥10 h. Therefore, our present study provides a novel strategy for the development of new TAM radicals with improved properties which should enable a wide range of biomedical *in vivo* EPR spectroscopy and imaging applications.

4. EXPERIMENTAL SECTION

General Information. All reactions were carried out under argon atmosphere. Anhydrous grade solvents were used for reactions and analytical grade solvents for purifications. All commercially available reagents were used as received without further purification. Chemical shifts (δ) are reported in parts per million (ppm) relative to the residual nondeuterated solvent peak in the corresponding spectra (chloroform δ = 7.27, D_2O δ = 2.48). The following abbreviations were used: s = singlet, d = doublet, t = triplet, m = multiplet. Coupling constants (J) were reported in Hz. UV–vis spectra were recorded in PB (phosphate buffer) or DMSO/PB (v/v = 1:1). High-resolution mass spectra (HRMS) were obtained on an MALDI-TOF spectrometer.

Synthesis of Compound 2. Compound **1** (2 g, 3.96 mmol) was dissolved into a mixture of 50 mL of DCM and 20 mL of 20% (w/v) aqueous Na_2CO_3 solution. 9-Fluorenylmethyl chloroformate (3.07 g, 11.87 mmol) dissolved into a small amount of DCM was added dropwise to the above reaction mixture under stirring. The resulting

DOI: 10.1021/acs.joc.6b02590
J. Org. Chem. 2017, 82, 588–596

reaction mixture was stirred for 16 h, solvent evaporated, and the crude product purified by silica column (4:1 hexane/EtOAc) to yield a colorless oil (2.62 g, 91%).

General Procedure for the Synthesis of 3. Compound **2** (6 g, 8.22 mmol) was dissolved into 15 mL of formic acid and stirred overnight after which the formic acid was removed under reduced pressure to yield a colorless oil **Fmoc-TA** (4.68 g, quant.).

Fmoc-TA (1 equiv), BOP (6 equiv), HOBt (6 equiv), and DIPEA (6 equiv) were dissolved in 40 mL of dry DCM, and the mixture was stirred for 30 min at room temperature. Then, mPEG (average molecular weight, 350 or 750) was added. The mixture was left refluxing for 2 days. The reaction was washed with 5% citric acid solution (w/v, 40 mL) and then saturated NaCl solution (40 mL), dried over anhydrous Na_2SO_4, and concentrated under vacuum. The crude product was purified by column chromatography on reverse phase C-18 using water followed by 0−60% methanol in water as eluants to afford compound **3**.

Compound 3a. Yield: 61% (2.04 g), colorless oil. ^{1}H NMR (400 MHz, $CDCl_3$) δ 7.76 (d, J = 7.6 Hz, 2H), 7.64 (d, J = 7.6 Hz, 2H), 7.40 (t, J = 7.2 Hz, 2H), 7.32 (t, J = 7.2 Hz, 2H), 5.43 (m, 1H), 4.29 (s, 2H), 4.22 (m, 6H), 4.20 (s, 1H), 3.68−3.63 (m, 111H), 3.56−3.54 (m, 6H), 3.38 (s, 9H), 2.58 (m, 6H).

Compound 3b. Yield: 45% (4.4 g), colorless oil. ^{1}H NMR (400 MHz, $CDCl_3$) δ 7.76 (d, J = 7.6 Hz, 2H), 7.64 (d, J = 7.4 Hz, 2H), 7.40 (t, J = 7.2 Hz, 2H), 7.32 (t, J = 7.4 Hz, 2H), 5.43 (s, 1H), 4.29 (s, 2H), 4.22 (t, J = 4.8 Hz, 6H), 4.18 (s, 1H), 3.66−3.63 (m, 214H), 3.56−3.54 (m, 6H), 3.38 (s, 9H), 2.59 (t, J = 6.2 Hz, 6H).

General Procedure for the Synthesis of 4. Compound **3** (1 equiv) dissolved into 5 mL of 20% piperidine in DCM was added. The mixture was stirred for 4 h, and solvent was evaporated and purified by silica column chromatography (gradient from 99:1 to 94:6 DCM/MeOH) to afford **4**.

Compound 4a. Yield: 75% (1.04 g), light yellow oil. ^{1}H NMR (400 MHz, $CDCl_3$) δ 4.28−4.17 (m, 6H), 3.81 (s, 2H), 3.71−3.66 (m, 90H), 3.38 (s, 9H), 3.31 (m, 6H), 2.59 (t, J = 6.4 Hz, 6H).

Compound 4b. Yield: 69% (1.25 g), colorless oil. ^{1}H NMR (400 MHz, $CDCl_3$) δ 4.27−4.25 (m, 6H), 3.74−3.64 (m, 197H), 3.56−3.54 (m, 6H), 3.38 (s, 9H), 2.63 (t, J = 6.7 Hz, 6H).

General Procedure for the Synthesis of 5. To a solution of **4** (1 equiv) in dry DCM (8 mL) was added solid K_2CO_3 (2 equiv). The resulting suspension was cooled to 0 °C, and bromoacetyl bromide (2 equiv) was added dropwise with stirring over the period of 0.5 h. The reaction mixture was allowed to warm to room temperature and stirred for 4 h. The reaction mixture was concentrated under vacuum. The resulting residue was purified by column chromatography on silica gel using eluting with DCM/MeOH = 99:1 to 93:7 as eluents to afford compound 5.

Compound 5a. Yield: 74% (812 mg), colorless oil. ^{1}H NMR (400 MHz, $CDCl_3$) δ 6.81 (s, 1H), 4.26−4.23 (m, 6H), 3.81 (s, 2H), 3.72−3.63 (m, 90H), 3.58−3.54 (m, 6H), 3.38 (s, 9H), 2.59 (t, J = 6.2 Hz, 6H).

Compound 5b. Yield: 75% (744 mg), colorless oil. ^{1}H NMR (400 MHz, $CDCl_3$) δ 6.79 (s, 1H), 4.26−4.23 (m, 6H), 3.81 (s, 2H), 3.71−3.62 (m, 188H), 3.56−3.54 (m, 6H), 3.38 (s, 9H), 2.59 (t, J = 6.4 Hz, 6H).

Compound 5c. Yield: 70% (1.7 g), colorless oil. ^{1}H NMR (400 MHz, $CDCl_3$) δ 4.33 (m, 2H), 3.89 (s, 2H), 3.65 (s, 57H), 3.55 (s, 2H), 3.38 (s, 3H).

Compound 5d. Yield: 76% (1.5 g), colorless oil. ^{1}H NMR (400 MHz, $CDCl_3$) δ 4.33 (m, 2H), 3.89 (s, 2H), 3.65 (s, 100H), 3.55 (s, 2H), 3.38 (s, 3H).

Synthesis of PEGylated TAM Radicals. Two different methods were used to synthesize these radicals (Scheme 2).

General Procedure of Method A. Cesium carbonate (3 equiv) was added to a solution of CT-03 (1 equiv) in 2 mL of anhydrous DMF. The resulting reaction mixture was stirred for 30 min at room temperature and then **5** (6 equiv) and KI (0.2 equiv) were added. The reaction mixture was continuously stirred under argon for 2 days. The solvent was evaporated under vacuum, and the crude product was purified by chromatography on silica gel with DCM/MeOH (99:1 to 9:1) as eluents to afford the final product.

TNP1. Yield, 85% (57 mg); purity, 97%; brown oil. ^{1}H NMR (400 MHz, $CDCl_3$): 4.23 (m, 18H), 3.73−3.63 (m, 279H), 3.56−3.53 (m, 18H), 3.38 (s, 27H), 2.59 (t, J = 6.2 Hz, 18H). ^{1}H NMR (400 MHz, D_2O): δ 4.22−4.17 (m, 7H), 3.67−3.59 (m, 146H), 3.28 (s, 27H), 2.58 (m, 10H). HRMS (MALDI-TOF): a broad peak from 4000 to 5400 (average $n \sim 7$).

d-TNP1. Yield: 85% (71 mg), brown oil. ^{1}H NMR (400 MHz, D_2O) 3.59 (m, 166), 3.27 (s, 27H). HRMS (MALDI-TOF): a broad peak from 4000 to 5400 (average $n \sim 7$).

TNP2. Yield, 80% (80 mg); purity, 97%; brown oil. ^{1}H NMR (400 MHz, D_2O) δ 4.17 (br, 11H), 3.59 (s, 454H), 3.27 (s, 27H), 2.58 (br, 11H). HRMS (MALDI-TOF): a broad peak from 4600 to 7600 (average $n \sim 16$).

TTP1. Yield, 86% (53 mg); purity, 97%; brown oil. ^{1}H NMR (400 MHz, D_2O) δ 3.59 (s, 109H), 3.27 (s, 9H). HRMS (MALDI-TOF): a broad peak from 2200 to 3700 (average $n \sim 16$).

TTP2. Yield, 84% (69 mg); purity, 96%; brown oil. ^{1}H NMR (400 MHz, D_2O) δ 3.59 (m, 136H), 3.27 (s, 9H). HRMS (MALDI-TOF): a broad peak from 3600 to 4600 (average $n \sim 22$).

General Procedure of Method B. Cesium carbonate (3 equiv) was added to a solution of CT03-OH (1 equiv) in 2 mL of anhydrous DMF. The resulting reaction mixture was stirred for 30 min at room temperature, and then **5** (6 equiv) and KI (0.2 equiv) were added. The reaction mixture was continuously stirred under argon for 2 days. The solvent was evaporated under vacuum, and the crude product was purified by chromatography on silica gel with DCM/MeOH (99:1 to 9:1) as eluents to afford **6**.

Compound 6a. Yield: 83% (136 mg), light red oil. ^{1}H NMR (400 MHz, $CDCl_3$) δ 6.79 (s, 1H), 4.23(m, 18H), 3.73−3.63 (m, 279H), 3.56−3.53 (m, 18H), 3.38 (s, 27H), 2.59 (t, J = 6.2 Hz, 18H), 1.78 (d, J = 12.1 Hz, 18H), 1.69 (s, 18H). ^{1}H NMR (400 MHz, D_2O) δ 4.22−4.17 (m, 18H), 3.67−3.59 (m, 292H), 3.53 (m, 18H), 3.28 (s, 27H), 2.58 (m, 18H), 1.63 (m, 36H).

Compound 6b. Yield: 80% (60.8 mg), light red oil. ^{1}H NMR (400 MHz, $CDCl_3$) δ 6.80 (s, 1H), 4.39−4.36 (m, 18H), 3.65 (m, 617H), 3.55 (m, 18H), 3.38 (s, 27H), 1.77 (d, J = 11.5 Hz, 18H), 1.68 (s, 18H).

Compound 6c. Yield: 85% (89.7 mg), light red oil. ^{1}H NMR (400 MHz, $CDCl_3$) δ 4.25−4.23 (m, 6H), 3.65 (m, 224H), 3.56−3.54 (m, 6H), 3.38 (s, 9H), 2.58 (t, J = 6.1 Hz, 6H), 1.77 (d, J = 11.3 Hz, 18H), 1.68 (s, 18H).

Compound 6d. Yield: 85% (74 mg), light red oil. ^{1}H NMR (400 MHz, $CDCl_3$) δ 6.73 (s, 1H), 4.32−4.29 (m, 6H), 3.58 (m, 298H), 3.49−3.47 (m, 6H), 3.31 (s, 9H), 1.72, 1.69 (d, J = 11.5 Hz, 18H), 1.61 (s, 18H).

A suspension of **6** in freshly distilled TFA (2 mL) and DCM (2 mL) was stirred at room temp under argon for 5 h. The solution was evaporated under vacuum and dried to afford the final compound (92%). See the above section for the characterization data of PEGylated TAM radicals.

Synthesis of d-TNP3. TAM radical d-TNP3 was synthesized using the previously reported method.[30] In brief, to a solution of dTdG[30] (50 mg, 23 μmol), HOBt (162 mg, 1.38 mmol), and EDCI (230 mg, 1.38 mmol) in D_2O (20 mL) and mPEG2000 (3.6 g, 2.07 mmol) was added DIPEA (209 μL, 1.38 mmol) under N_2 atmosphere. The reaction mixture was stirred at room temperature for 7 days, and then 20 mL of 5% citric acid solution was added. The resulting solution was dialyzed against water (7 × 1 L) with a molecular weight cutoff of 3000D and further purified by column chromatography on Sephadex G-50 using water as an eluent to give the PEGylated TAM radical d-TNP3 as a brown solid (219 mg, 55%). ^{1}H NMR (400 MHz, $CDCl_3$) δ 4.23−4.21 (m, 18H), 3.73−3.53 (m, 1773H), 3.56−3.54 (m, 18H), 3.38 (s, 27H), 2.58 (t, J = 6.2 Hz, 18H). HRMS (MALDI-TOF): a broad peak from 10 000 to 20 000. The paramagnetic purity of d-TNP3 was determined by EPR using CT-03 as standard to be 86%. According to NMR analysis (see the ^{1}H NMR spectrum of d-TNP3 in the Supporting Information), the impurity in the sample of d-TNP3

DOI: 10.1021/acs.joc.6b02590
J. Org. Chem. 2017, 82, 588−596

was only free mPEG 2000, which has good biocompatibility and will not significantly interfere with the biological applications of d-TNP3.

Determination of the Paramagnetic Purity. The paramagnetic purities of PEGylated TAM radicals were determined by EPR using CT-03 as standard.[19] In a typical experiment, purified TAM radical was weighed and dissolved in DMSO/water (v/v = 1:1). The EPR spectrum was obtained, and the corresponding peak area was determined using double integration (Figure S1). The concentration of the TAM radical was then determined using a standard curve of known concentration of CT-03 versus peak area (Figure S2 and Table S1). Each experiment was done in triplicate. The paramagnetic purity of each PEGylated TAM radical was determined to be >95% except for d-TNP3 (86%).

Measurement of Octanol–Water Partition Coefficient (LogP). Solutions of TAM radicals with various concentrations (10–50 μM) in octanol-saturated PB (20 mM, pH 7.4) were prepared and their UV–vis spectra were recorded. Then, the absorption intensities at 496 nm (TTP1, TNP2, TNP1, and TNP2) or at 484 nm (ET-03) were plotted as a function of concentrations (Figure S14). Subsequently, solutions (0.5 mL) of TAM radicals in octanol-saturated PB (20 mM, pH 7.4) were incubated with PB-saturated octanol (0.5 mL) for 3 h at room temperature. Two phases were separated by centrifugation and their UV–vis absorbance intensities at 496 nm (TTP1, TNP2, TNP1 and TNP2) or at 484 nm (ET-03) in the PB were measured. The concentrations of these radicals in both phases were calculated according to the plot in Figure S14 and their octanol–water partition coefficients were obtained. All the experiments were carried out in triplicate. The detailed results are shown in Table S4.

EPR Experiments and Spectral Simulation. *In vitro* EPR measurements were carried out on an X-band spectrometer at room temperature. General instrumental settings were as follows: modulation frequency, 30–100 kHz; microwave power, 0.1–5 mW; modulation amplitude, 0.01–1 G. Measurements were performed in 50 μL capillary tubes. EPR spectral simulation of TAM radicals was conducted by the WINSIM program. The parameters used for ET-03, TTP1, TTP2, TNP1, and TNP2 were shown in Table 2.

Stability Studies toward Biological Oxidoreductants. Solutions of GSH (1 mM), Asc (1 mM), and H_2O_2 (1 mM) in PB (pH 7.4, 20 mM) were used. The Fe(II)–NTA complex was prepared by dissolving $(NH_4)_2Fe(SO_4)_2$ and NTA with a molar ratio of 1:2 in water under anaerobic conditions. The Fe(III)–NTA solution (Fe/NTA 1:2) was prepared by slow addition of the appropriate volume of acidic Fe(III) stock solution into a vigorously stirred solution of NTA in water. The resulting solution was slowly neutralized to pH 7.4 using 0.1 M NaOH. Either Fe(II)–NTA or Fe(III)–NTA solution was freshly prepared before use. Hydroxyl radical ($HO^{\bullet}$) was continuously generated from the system consisting of Fe(III)–NTA (0.1 mM) and H_2O_2 (1 mM). Superoxide was generated using the xanthine (X)/xanthine oxidase (XO) system using XO (20 mU/mL) and X (0.4 mM) in the presence of DTPA (0.1 mM). Alkylperoxyl radical was generated by thermolysis of 2,2′-azobis-2- methylpropanimidamide, dihydrochloride (AAPH, 1 mM) at 37 °C. EPR spectra were recorded 30 min after mixing the TAM radical solution (20 μM) with various oxidoreductants. Effect of various reactive species on TAM radicals was expressed as percentage of TAM radical remaining after exposure to reactive species for 30 min which was obtained by the double integral of the EPR signal. Each experiment was conducted three times.

Preparation of Liver Homogenate and Blood of Rat. On the day of the experiments, 1 mL of blood was taken by retro-orbital bleed of rats, and then 125 μL of heparin solution (1% w/v) was added. The resulting blood was stocked on ice for the subsequent use. The rat was then sacrificed and livers were taken. Rat livers were weighed and cut into small pieces and washed with PB (20 mM, pH 7.4) to remove blood. The resulting liver pieces were blotted with paper towels and then transferred to a homogenizer. Thereafter, a 4-fold volume of PB (20 mM, pH 7.4) was added to the homogenizer, and the liver pieces were manually ground. The resulting homogenate was centrifuged at 4000 rpm at 4 °C for 15 min and the upper suspension was taken for the stability analysis. All animal experiments were carried out according to the protocols approved by the Tianjin Medical University Animal Care and Use Committee.

***In Vivo* L-Band EPR Measurement.** Male C57Bl6 mice of ~30 g of weight were anesthetized with isoflurane inhalation and a jugular venous catheter placed. Tail cuff blood pressure monitoring (Coda noninvasive blood pressure system, Kent Scientific) measured systolic blood pressures of ~100/70 with heart rate of ~450 beats per minute prior to the start of the infusion and with repeat measurements postinfusion similar values were obtained. With intravenous infusion in the jugular vein of ~0.2 mmol/kg of d-TNP3 in 0.3 mL of normal saline over 180 s, no acute toxicity was seen with stable respiratory and heart rate. EPR measurements were performed with a Magnettech L-band spectrometer with a center field of 462.99 G, scan width of 3.9 G, modulation amplitude of 100 mG, microwave power of 25 mW, time constant of 300 ms, and scan time of 30 s using a surface coil resonator placed over the right thigh of the mouse.

■ ASSOCIATED CONTENT

Supporting Information

The Supporting Information is available free of charge on the ACS Publications website at DOI: 10.1021/acs.joc.6b02590.

^{1}H NMR, HRMS, EPR, and UV–vis spectra; experimental procedures for measurement of LogP; self-aggregation concentrations; binding with BSA; as well as stability of TAM radicals in rat liver homogenate and blood (PDF)

■ AUTHOR INFORMATION

Corresponding Authors

*E-mail: liuyangping@tmu.edu.cn.

*E-mail: jay.zweier@osumc.edu.

ORCID

Yangping Liu: 0000-0001-5455-3602

Notes

The authors declare no competing financial interest.

■ ACKNOWLEDGMENTS

This work was partially supported by the National Natural Science Foundation of China (Grants 81201126, 21572161, and 31500684), Tianjin Research Program of Application Foundation and Advanced Technology (Grants 15JCZDJC32300 and 15JCYBJC23700), and NIH Grant EB016096.

■ REFERENCES

(1) Gomberg, M. *J. Am. Chem. Soc.* **1900**, *22*, 757–771.

(2) Ardenkjær-Larsen, J. H.; Laursen, I.; Leunbach, I.; Ehnholm, G.; Wistrand, L. G.; Petersson, J. S.; Golman, K. *J. Magn. Reson.* **1998**, *133*, 1–12.

(3) Reddy, T. J.; Iwama, T.; Halpern, H. J.; Rawal, V. H. *J. Org. Chem.* **2002**, *67*, 4635–4639.

(4) Williams, B. B.; al Hallaq, H.; Chandramouli, G. V.; Barth, E. D.; Rivers, J. N.; Lewis, M.; Galtsev, V. E.; Karczmar, G. S.; Halpern, H. J. *Magn. Reson. Med.* **2002**, *47*, 634–638.

(5) Elas, M.; Ahn, K. H.; Parasca, A.; Barth, E. D.; Lee, D.; Haney, C.; Halpern, H. J. *Clin. Cancer Res.* **2006**, *12*, 4209–4217.

(6) Lurie, D. J.; Li, H. H.; Petryakov, S.; Zweier, J. L. *Magn. Reson. Med.* **2002**, *47*, 181–186.

(7) Krishna, M. C.; English, S.; Yamada, K.; Yoo, J.; Murugesan, R.; Devasahayam, N.; Cook, J. A.; Golman, K.; Ardenkjaer-Larsen, J. H.; Subramanian, S.; Mitchell, J. B. *Proc. Natl. Acad. Sci. U. S. A.* **2002**, *99*, 2216–2221.

(8) Hyodo, F.; Murugesan, R.; Matsumoto, K.; Hyodo, E.; Subramanian, S.; Mitchell, J. B.; Krishna, M. C. *J. Magn. Reson.* **2008**, *190*, 105–112.

DOI: 10.1021/acs.joc.6b02590
J. Org. Chem. 2017, 82, 588–596

(9) Gallagher, F. A.; Kettunen, M. I.; Day, S. E.; Hu, D. E.; Ardenkjaerlarsen, J. H.; Ri, Z.; Jensen, P. R.; Karlsson, M.; Golman, K.; Lerche, M. H. *Nature* **2008**, *453*, 940−943.
(10) Sriram, R.; Kurhanewicz, J.; Vigneron, D. B. Hyperpolarized Carbon-13 MRI and MRS Studies. In *eMagRes*; John Wiley & Sons, Ltd.: Chichester, U.K., 2014; pp 311−324, DOI: 10.1002/9780470034590.emrstm1253
(11) Dhimitruka, I.; Velayutham, M.; Bobko, A. A.; Khramtsov, V. V.; Villamena, F. A.; Hadad, C. M.; Zweier, J. L. *Bioorg. Med. Chem. Lett.* **2007**, *17*, 6801−6805.
(12) Rogozhnikova, O. Y.; Vasiliev, V. G.; Troitskaya, T. I.; Trukhin, D. V.; Mikhalina, T. V.; Halpern, H. J.; Tormyshev, V. M. *Eur. J. Org. Chem.* **2013**, *2013*, 3347−3355.
(13) Decroos, C.; Prange, T.; Mansuy, D.; Boucher, J. L.; Li, Y. *Chem. Commun.* **2011**, *47*, 4805−4807.
(14) Tormyshev, V. M.; Rogozhnikova, O. Y.; Bowman, M. K.; Trukhin, D. V.; Troitskaya, T. I.; Vasiliev, V. G.; Shundrin, L. A.; Halpern, H. J. *Eur. J. Org. Chem.* **2014**, *2014*, 371−380.
(15) Driesschaert, B.; Charlier, N.; Gallez, B.; Marchand-Brynaert, J. *Bioorg. Med. Chem. Lett.* **2008**, *18*, 4291−4293.
(16) Charlier, N.; Driesschaert, B.; Wauthoz, N.; Beghein, N.; Préat, V.; Amighi, K.; Marchand-Brynaert, J.; Gallez, B. *J. Magn. Reson.* **2009**, *197*, 176−180.
(17) Driesschaert, B.; Leveque, P.; Gallez, B.; Marchand-Brynaert, J. *Tetrahedron Lett.* **2013**, *54*, 5924−5926.
(18) Driesschaert, B.; Leveque, P.; Gallez, B.; Marchand-Brynaert, J. *Eur. J. Org. Chem.* **2014**, *2014*, 8077−8084.
(19) Liu, Y. P.; Villamena, F. A.; Sun, J.; Xu, Y.; Dhimitruka, I.; Zweier, J. L. *J. Org. Chem.* **2008**, *73*, 1490−1497.
(20) Liu, Y. P.; Villamena, F. A.; Sun, J.; Wang, T. Y.; Zweier, J. L. *Free Radical Biol. Med.* **2009**, *46*, 876−883.
(21) Liu, Y. P.; Song, Y. G.; De Pascali, F.; Liu, X. P.; Villamena, F. A.; Zweier, J. L. *Free Radical Biol. Med.* **2012**, *53*, 2081−2091.
(22) Driesschaert, B.; Marchand, V.; Leveque, P.; Gallez, B.; Marchand-Brynaert, J. *Chem. Commun.* **2012**, *48*, 4049−4051.
(23) Bobko, A. A.; Dhimitruka, I.; Komarov, D. A.; Khramtsov, V. V. *Anal. Chem.* **2012**, *84*, 6054−6060.
(24) Dhimitruka, I.; Bobko, A. A.; Eubank, T. D.; Komarov, D. A.; Khramtsov, V. V. *J. Am. Chem. Soc.* **2013**, *135*, 5904−5910.
(25) Liu, Y. P.; Song, Y. G.; Rockenbauer, A.; Sun, J.; Hemann, C.; Villamena, F. A.; Zweier, J. L. *J. Org. Chem.* **2011**, *76*, 3853−3860.
(26) Liu, Y. P.; Villamena, F. A.; Rockenbauer, A.; Zweier, J. L. *Chem. Commun.* **2010**, *46*, 628−630.
(27) Yang, Z. Y.; Liu, Y. P.; Borbat, P.; Zweier, J. L.; Freed, J. H.; Hubbell, W. L. *J. Am. Chem. Soc.* **2012**, *134*, 9950−9952.
(28) Shevelev, G. Y.; Krumkacheva, O. A.; Lomzov, A. A.; Kuzhelev, A. A.; Rogozhnikova, O. Y.; Trukhin, D. V.; Troitskaya, T. I.; Tormyshev, V. M.; Fedin, M. V.; Pyshnyi, D. V.; Bagryanskaya, E. G. *J. Am. Chem. Soc.* **2014**, *136*, 9874−9877.
(29) Mathies, G.; Caporini, M. A.; Michaelis, V. K.; Liu, Y. P.; Hu, K. N.; Mance, D.; Zweier, J. L.; Rosay, M.; Baldus, M.; Griffin, R. G. *Angew. Chem., Int. Ed.* **2015**, *54*, 11770−11774.
(30) Song, Y. G.; Liu, Y. P.; Hemann, C.; Villamena, F. A.; Zweier, J. L. *J. Org. Chem.* **2013**, *78*, 1371−1376.
(31) Song, Y.; Liu, Y.; Liu, W.; Villamena, F. A.; Zweier, J. L. *RSC Adv.* **2014**, *4*, 47649−47656.
(32) Slashed, R. M. J. O.; Rise, F.; Andersson, S.; Almen, T.; Golman, K. *Triarylmethyl radicals and the use of inert carbon free radicals in MRI*. U.S. Patent 5,599,522, February 4, 1997.
(33) Leunbach, I.; Ardenkjaer-Larsen, J. H. *Method for determining oxygen concentration using magnetic resonance imaging*. U.S. Patent 5,765,562, June 16, 1998.
(34) Andersson, S.; Radner, F.; Rydbeck, A.; Servin, R.; Wistrand, L. G.; Thaning, M. *Free radicals comprising benzodithiole derivatives*. U.S. Patent 6,063,360, May 16, 2000.
(35) Li, H.; Deng, Y.; He, G.; Kuppusamy, P.; Lurie, D. J.; Zweier, J. L. *Magn. Reson. Med.* **2002**, *48*, 530−534.
(36) Frank, J.; Elewa, M.; M, M. S.; El Shihawy, H. A.; El-Sadek, M.; Mueller, D.; Meister, A.; Hause, G.; Drescher, S.; Metz, H. *J. Org. Chem.* **2015**, *80*, 6754−6766.
(37) Abbas, K.; Boutier-Pischon, A.; Auger, F.; Françon, D.; Almario, A.; Frapart, Y. M. *J. Magn. Reson.* **2016**, *270*, 147−156.
(38) Kaminskas, L. M.; Kelly, B. D.; McLeod, V. M.; Boyd, B. J.; Krippner, G. Y.; Williams, E. D.; Porter, C. J. H. *Mol. Pharmaceutics* **2009**, *6*, 1190−1204.
(39) Le Devedec, F.; Strandman, S.; Hildgen, P.; Leclair, G.; Zhu, X. X. *Mol. Pharmaceutics* **2013**, *10*, 3057−3066.
(40) Herzberger, J.; Niederer, K.; Pohlit, H.; Seiwert, J.; Worm, M.; Wurm, F. R.; Frey, H. *Chem. Rev.* **2016**, *116*, 2170−2243.
(41) Ulbrich, K.; Holá, K.; Šubr, V.; Bakandritsos, A.; Tuček, J.; Zbořil, R. *Chem. Rev.* **2016**, *116*, 5338−5431.
(42) Rajca, A.; Wang, Y.; Boska, M.; Paletta, J. T.; Olankitwanit, A.; Swanson, M. A.; Mitchell, D. G.; Eaton, S. S.; Eaton, G. R.; Rajca, S. *J. Am. Chem. Soc.* **2012**, *134*, 15724−15727.
(43) Sowers, M. A.; Mccombs, J. R.; Wang, Y.; Paletta, J. T.; Morton, S. W.; Dreaden, E. C.; Boska, M. D.; Ottaviani, M. F.; Hammond, P. T.; Rajca, A. *Nat. Commun.* **2014**, *5*, 5460−5460.
(44) Cardona, C. M.; Gawley, R. E. *J. Org. Chem.* **2002**, *67*, 1411−1413.
(45) Tormyshev, V. M.; Genaev, A. M.; Sal'nikov, G. E.; Rogozhnikova, O. Y.; Troitskaya, T. I.; Trukhin, D. V.; Mamatyuk, V. I.; Fadeev, D. S.; Halpern, H. J. *Eur. J. Org. Chem.* **2012**, *2012*, 623−629.
(46) Dhimitruka, I.; Grigorieva, O.; Zweier, J. L.; Khramtsov, V. V. *Bioorg. Med. Chem. Lett.* **2010**, *20*, 3946−3949.
(47) Decroos, C.; Balland, V.; Boucher, J. L.; Bertho, G.; Yun, X. L.; Mansuy, D. *Chem. Res. Toxicol.* **2013**, *26*, 1561−1569.
(48) Driesschaert, B.; Robiette, R.; Lucaccioni, F.; Gallez, B.; Marchandbrynaert, J. *Chem. Commun.* **2011**, *47*, 4793−4795.
(49) Ortiz, A.; Flora, W. H.; D'Ambruoso, G. D.; Armstrong, N. R.; McGrath, D. V. *Chem. Commun.* **2005**, 444−446.
(50) Decroos, C.; Li, Y.; Bertho, G.; Frapart, Y.; Mansuy, D.; Boucher, J. L. *Chem. Res. Toxicol.* **2009**, *22*, 1342−1350.

DOI: 10.1021/acs.joc.6b02590
J. Org. Chem. 2017, 82, 588−596